Subpicosecond Solvent Dynamics in Charge-Transfer Transitions: Challenges and Opportunities in Resonance Raman Spectroscopy

JEANNE L. MCHALE*
Department of Chemistry, University of Idaho, Moscow, Idaho 83844-2343

Received June 20, 2000

ABSTRACT
Resonance Raman spectroscopy is an established tool for the determination of structure and dynamics in electronically excited states. In condensed-phase systems, Raman excitation profiles and electronic absorption spectra depend on changes in molecular geometry and solvation structure induced by electronic excitation. Recent studies of solvent isotope effects on resonance Raman intensities in charge-transfer excitations reveal solvent dynamics taking place on a subpicosecond time scale and vibrational mode-specific solute−solvent interactions. These discoveries present challenges to the current working theories for analysis of resonance Raman and absorption spectra.

1. Introduction: Resonance Raman Intensity Analysis

Resonance Raman and electronic absorption spectroscopy are intimately connected experiments which provide a window on the intramolecular and solvent dynamics that accompany an electronic transition.[1−5] Electron transfer is a recurring motif in chemistry and biology, and charge-transfer transitions continue to hold the interest of spectroscopists.[6] Resonance Raman spectroscopy has been applied[7] to the determination of solvent and internal reorganization energies which influence the rate constant for return electron transfer. The importance of solvent relaxation in electron transfer has been highlighted by a number of experimental[8−10] and theoretical[11,12] studies. This Account discusses our recent use of solvent isotopic substitution to focus on solvent dynamical effects on charge-transfer transitions as revealed by resonance Raman intensities.[13−17]

The vibrational modes coupled to electron transfer are those which correlate with the geometry change of the molecule. These Franck−Condon active modes are enhanced in the resonance Raman (RR) spectrum and contribute to the breadth of the electronic absorption spectrum. The equilibrium geometry along the normal coordinate Q_a of an active mode is displaced in the excited state, as shown in Figure 1, causing the electronic absorption to be distributed over a range of energies associated with transitions to different final vibrational states. Immediately after the vertical transition, the molecule is still in the equilibrium geometry of the ground electronic state. The additional energy of the molecule compared to that of the excited-state equilibrium geometry is called the internal reorganization energy, λ_{int}, and it may be resolved into contributions λ_a from each of the displaced modes. The greater the displacement of the upper-state potential energy surface relative to the ground state surface, the more different are the values of the 0−0 energy ΔE_0 and the vertical energy ΔE_{vert}, and the broader is the absorption spectrum. The intensity of a vibrational mode in the RR spectrum increases with increasing mode displacement. For solution-phase molecules with a large number of Franck−Condon active normal modes, spectral congestion and solvent broadening conceal the vibrational progression in the absorption spectrum. The resonance Raman spectrum, however, reveals the frequencies of the hidden vibrational modes, and through analysis of the absolute RR intensities the normal mode displacements are uncovered. The key to this analysis is the measurement of Raman intensities as a function of excitation frequency for each active mode. These are known as Raman excitation profiles (REPs).

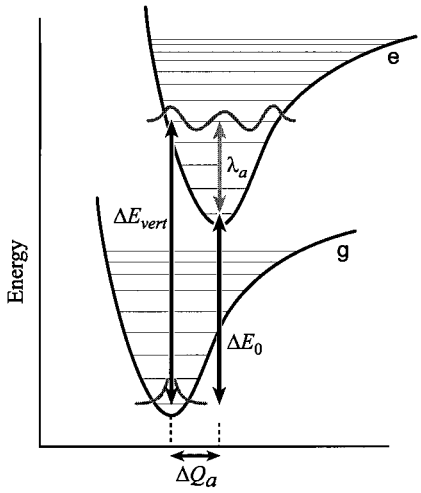

FIGURE 1. Ground- and excited-state potential energy as a function of normal coordinate. ΔE_0 is the 0−0 transition energy, and the vertical energy ΔE_{vert} is the transition energy for the molecule fixed at the ground-state equilibrium geometry. ΔQ_a is the displacement of the excited-state potential curve, relative to the ground-state curve, along the normal coordinate Q_a, and λ_a is the contribution of mode *a* to the internal reorganization energy.

Electronic transitions may also be accompanied by a change in the equilibrium configuration of the surrounding solvent, particularly for charge-transfer transitions. For example, a large change in dipole moment on excitation induces the solvent reorganization pictured in Figure 2. The ground and excited electronic states of the chromophore are displaced along the "solvent coordinate", which

Jeanne L. McHale was born in Baltimore, MD, in 1953. She obtained a bachelor's degree in chemistry at Wright State University in Ohio, and attended graduate school at the University of Utah, where she obtained the Ph.D. in physical chemistry in 1979 under the direction of Prof. Jack Simons. After postdoctoral work with Prof. Jim Wang at Utah, she joined the faculty of chemistry at the University of Idaho in 1980, where she is Professor of Chemistry and continues to indulge her longstanding interest in the spectroscopy of charge-transfer systems. She is a fellow in the American Association for the Advancement of Science and the author of *Molecular Spectroscopy*.

10.1021/ar000071 CCC: $20.00
Published on Web 01/11/2001

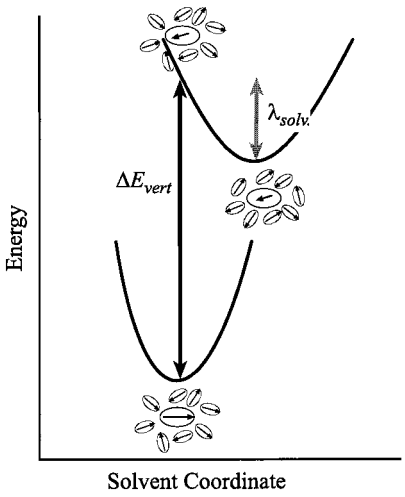

FIGURE 2. Ground- and excited-state potential energy as a function of solvent coordinate. The arrows depict the dipole moments of the solute and surrounding solvent molecules in the ground and excited electronic states.

for polar solvents can be visualized as a collective orientational coordinate. The solvent reorganization energy λ_{solv} is the energy lost by the solvent molecules as they relax from the strained vertical configuration to the configuration equilibrated to the excited-state charge distribution.

Both internal reorganization energy and solvent reorganization energy contribute to the spectral width as well as the Stokes shift of the relaxed fluorescence spectrum. When the spectra are structureless, it is not possible to distinguish the influence of solvent reorganization from that due to internal modes. However, the two effects have very different consequences on the resonance Raman spectrum. While increasing internal reorganization results in increased RR intensity, the effect of increasing solvent reorganization is to diminish RR intensities. To understand how absorption and resonance Raman spectroscopy reveal excited-state dynamics, the theoretical foundations are presented in the next section, followed by results from our solvent isotope studies in section 3. These results have serious implications for conventional approaches to modeling absorption and Raman profiles, prompting consideration of improved approaches discussed briefly in section 4.

2. Theory of Absorption and Resonance Raman Excitation Profiles

The absorption maximum occurs at the energy of the vertical transition $\Delta E_{vert} = h\nu_{max,abs}$, which is the sum of the 0−0 energy and the internal and solvent reorganization energies. Conversely, relaxed fluorescence originates from the equilibrium solvent/solute geometry of the excited electronic state, i.e., the minima in the upper potential energy curves of Figures 1 and 2. The maximum in the fluorescence spectrum occurs at an energy which is less than the 0−0 energy due to reorganization of the molecule and surrounding solvent as they relax to their ground-state equilibrium positions. If the upper and lower curves in Figures 1 and 2 are the same shape, and merely displaced horizontally, then the ground- and excited-state reorganization energies are the same. The solvent response and normal modes are then said to be *linearly* coupled to the transition. When linear coupling holds, the fluorescence and absorption spectra are mirror images of one another, and the total reorganization energy is half of the Stokes shift between absorption and fluorescence peak frequencies. Alas, fluorescence is the enemy of resonance Raman spectroscopy, and in our work the absorption and fluorescence profiles are never mirror images of one another! We consider molecules for which the Stokes shift, $\nu_{max,abs} - \nu_{max,fluor}$, is large enough to permit RR spectra to be determined without interference from fluorescence. This implies large solvent and/or internal reorganization energy. Large values of λ_{solv} are typical of charge-transfer transitions. Since the charge distributions in the ground and excited electronic states are very different, the solvent response may depend on the electronic state of the solute. Large values of λ_{int} imply very different ground- and excited-state geometries of the solute. There is also the problem of separating the total reorganization energy into internal and solvent contributions. This is where time-dependent approaches to analysis of absorption and resonance Raman profiles can help.

The time-dependent theory of spectroscopy[1−5] has been widely reviewed in this journal and others, so only a brief summary is given. In this theory, the absorption cross section σ_A is found as follows:

$$\sigma_A(\omega_0) = \frac{2\pi(\mu_{ge}^0)^2\omega_0}{3\hbar cn}\sum_i P_i \int_{-\infty}^{\infty}\langle i|i(t)\rangle \exp[i(\omega_i + \omega_0)t] \times \exp[-g(|t|)]\, dt \quad (1)$$

and the Raman cross section for the $i \rightarrow f$ transition is given by

$$\sigma_{R,i\rightarrow f}(\omega_0) = \frac{8\pi\omega_s^3\omega_0(\mu_{ge}^0)^4}{9\hbar^2c^4}\sum_i P_i \left|\int_0^{\infty}\langle f|i(t)\rangle \times \exp[i(\omega_i + \omega_0)t] \exp[-g(t)]\, dt\right|^2 \quad (2)$$

In these equations, ω_0 is the incident frequency, ω_s is the scattered light frequency, $\hbar\omega_i$ is the energy of the initial state i, μ_{eg}^0 is the transition moment at the ground-state equilibrium geometry (Condon approximation), n is the refractive index of the solution, c is the speed of light, and $\hbar$ is Planck's constant divided by 2π. The integrands contain time-dependent overlaps of the initial multimodal vibrational state $|i(t)\rangle$, which evolves on the upper potential surface, projected onto the time-zero initial state $|i\rangle$, in absorption, or final state $|f\rangle$, for Raman. The summation over the Boltzmann probability P_i accounts for a thermal distribution of initial states. Closed-form expressions for the time-dependent overlaps $\langle i|i(t)\rangle$ and $\langle f|i(t)\rangle$ depend on the frequencies ω_a and dimensionless displacements Δ_a of the active vibrational modes.[5] The internal reorganiza-

tion energy is found from the fitted displacements:

$$\lambda_{\text{int}} = \sum_{\text{a}} \lambda_{\text{a}} = \frac{1}{2} \sum_{a} \Delta_{\text{a}}^2 \nu_{\text{a}} \tag{3}$$

Our focus here is on the influence of solvent-induced dephasing which is accounted for by the exponential function of $g(t)$. This function captures the effect of the solvent on the electronic transition and vice versa, and by adjusting the parameters on which it depends the solvent reorganization energy may be determined.

Solvent-induced pure dephasing is spectral broadening that results from time-dependent perturbations to the electronic transition frequency ω_{eg} due to fluctuating solvent−solute interactions. The time correlation function for the fluctations in the electronic transition frequency is defined as

$$\text{M(t)} \equiv \frac{\langle \delta\omega_{\text{eg}}(\text{t}) \delta\omega_{\text{eg}}(0) \rangle}{\langle (\delta\omega_{\text{eg}})^2 \rangle} \equiv \frac{\text{C(t)}}{\text{D}^2} \tag{4}$$

The angle brackets in this equation signify an equilibrium average over the solvent coordinates. When linear solvent response applies, this average is independent of the electronic state of the solute. The amplitude D determines the solvent broadening of the absorption spectrum as well as the solvent reorganization energy.

$$\lambda_{\text{solv}} = \frac{D^2}{2k_{\text{B}}T} \tag{5}$$

As has been shown by Mukamel and co-workers,[18−20] a closed-form integral expression enables $g(t)$ to be found from the correlation function $M(t)$. The problem is that we must resort to models for the correlation function. The Brownian oscillator model, which assumes that frequency fluctations relax exponentially, $M(t) = \exp(-\Lambda t)$, leads to a convenient expression for $g(t)$ which depends on only two parameters, the rate Λ and amplitude D of the frequency fluctuations. This model is based on assumptions which are in conflict with experimental information for many charge-transfer systems. It assumes a linear solvent response and that the Stokes shift is much smaller than the absorption line width. The functional form for $M(t)$ is not valid on the subpicosecond time scale relevant to the RR experiment. Both theory[21] and experiment[22−24] have shown that the initial phase of solvent relaxation is a Gaussian function of time, reflecting a period of free inertial rotation on a time scale of less than 100 fs for small molecules. This is followed by exponential decay on a picosecond time scale, characteristic of diffusional motion. Still more complex dynamics are observed in alcohol solutions, for which hydroxyl group torsions and dynamics of hydrogen bonds are observed at intermediate time scales. Several time domain spectroscopy experiments, such as time-resolved fluorescence and three-pulse stimulated photon echo, determine $M(t)$ directly.[25−27] Thus, there is a great deal of experimental data to guide the modeling of $M(t)$, but it should be kept in mind that different chromophores project out different parts of the solvent response.

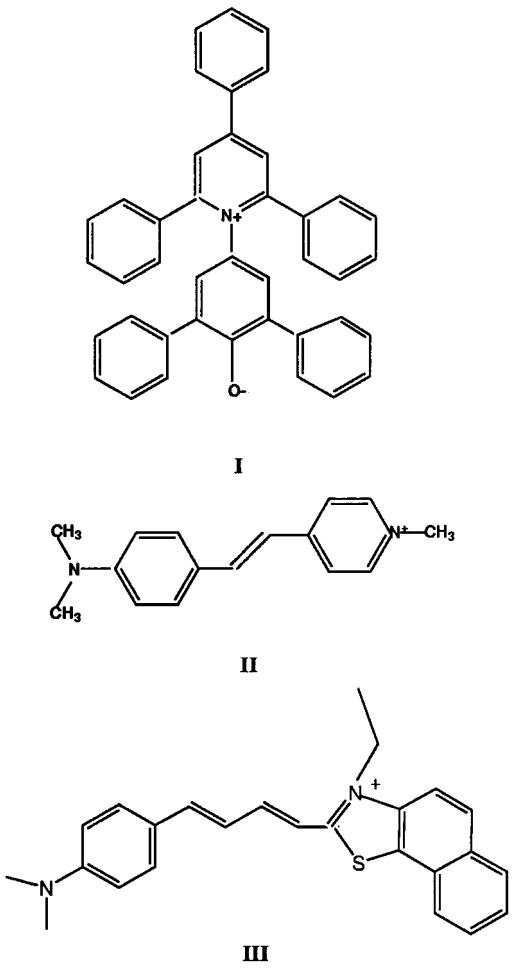

FIGURE 3. Molecules used in resonance Raman studies of solvent dynamics. **I**, Betaine-30; **II**, HR; **III**, LDS750.

Several key assumptions are employed to arrive at and apply eqs 1 and 2. The first is that the dephasing of the electronic transition is independent of vibrational state. Another practical assumption, consistent with the idea of linear solvent response, is that the $g(t)$ employed to account for dephasing in the evaluation of σ_{A} is the same $g(t)$ on which the Raman cross section σ_{R} depends. In the next section we present experimental results that call into question these assumptions.

3. Solvent Isotope Effects in Resonance Raman Spectroscopy

The molecules which we have employed as probes for RR studies of solvent dynamics, shown in Figure 3, represent a range of solvent isotope effects as discussed below.

3.1. Betaine-30: Solvatochromism and Solvent Dynamics. The $S_0 \rightarrow S_1$ transition of betaine-30 (**I** in Figure 3) has been widely used as an empirical measure of solvent polarity.[28] Recent studies have employed time domain spectroscopy[8−10] and computer simulations[29,30] to investigate solvent effects on the electron transfer and spectra. Quantum calculations incorporating solvent effects have also been reported.[31] The blue shift of the

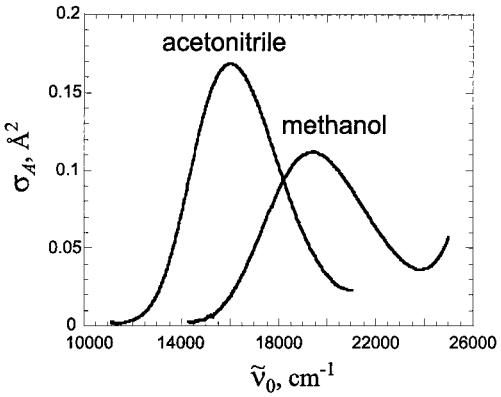

FIGURE 4. Absorption spectrum of betaine-30 in acetonitrile and methanol.

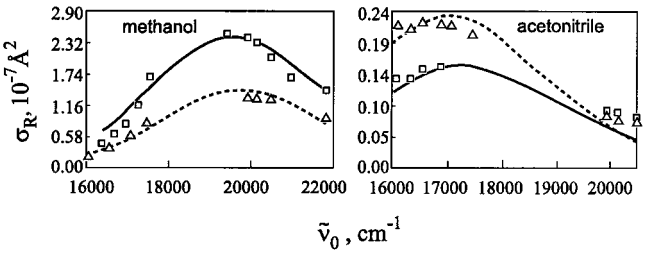

FIGURE 5. Raman excitation profiles of the 1622 cm^{-1} mode of betaine-30 in methanol and acetonitrile. The squares are for data in deuterated solvent and the triangles are for those in protiated solvent. The curves are calculated using time-dependent theory as described in refs 13 and 14.

absorption spectrum with increasing solvent polarity derives from the larger dipole moment in the ground state (15 D) compared to that in the excited state (6 D).[32]

We determined Raman excitation profiles for betaine-30 in acetonitrile,[13] methanol,[14] and their perdeuterated derivatives, at wavelengths spanning the visible absorption band. These two solvents were chosen because they have similar bulk dielectric properties, but due to hydrogen bonding the charge-transfer band is blue-shifted in methanol compared to that in acetonitrile, as shown in Figure 4. The absorption spectrum in either solvent is independent of solvent isotopomer. Similarly, the betaine-30 peak frequencies in the RR spectrum are independent of solvent and solvent isotopomer, with the exception of a mode observed at 1316 cm^{-1} in CH_3OH which shifts to 1320 cm^{-1} in CD_3OD. This mode appears to correlate with one observed at 1295 cm^{-1} in both CH_3CN and CD_3CN. We assume this vibration involves C−O stretching and is sensitive to hydrogen bonding. For the most part there are no solvent- or solvent isotopomer-induced perturbations to the ground-state structure of betaine-30. Thus, the solvent isotope effects we observed on the RR intensities are reporting details of the excited electronic state!

Example Raman profiles for betaine-30 are shown in Figure 5. In acetonitrile, Raman intensities are generally smaller in deuterated and then protiated solvent, while in methanol the reverse is true. Furthermore, the magnitude of the solvent isotope effect varies with normal mode. Some of the lower frequency modes, in the range 200−400 cm^{-1}, are particularly sensitive to solvent isotopomer. Comparison of the results in acetonitrile and methanol is also interesting. The general trend is that Raman intensities are about an order of magnitude lower in acetonitrile than in methanol, even though the transition moment is greater in acetonitrile. For a given normal mode, the influence of isotopic substitution is solvent dependent. For example, the betaine-30 vibration at 645 cm^{-1} is fairly independent of solvent isotope in methanol, but much less intense in deuterated than in protiated acetonitrile.

How do we understand these results? The excited-state geometries are not expected to depend on solvent isotopomer; therefore, the Raman intensities are revealing the influence of solvent dynamics. In comparing the general trends in methanol to those in acetonitrile, it is clear that the very different amplitudes of solvent relaxation have a strong influence on the Raman cross sections. Acetonitrile is a particularly "fast" solvent: the ∼70−110 fs inertial phase accounts for more than half of the total solvent relaxation.[33−35] In CH_3OH, as in other alcohols, the solvent response is more complex,[36−38] but the amplitude of the inertial phase is smaller than that in CH_3CN.

To model the betaine-30 data, we employed a solvent-induced dephasing function based on a bimodal solvent response comprising a fast (presumably inertial) and a slow (diffusional) phase of relaxation. Each phase of relaxation was characterized by an amplitude and rate and was taken to be exponential. The exponential form is not strictly correct because the fast phase ought to decay as $\exp(-t^2)$, but it was chosen because it leads to a simple expression for the solvent-dephasing function $g(t)$. Our best fit to the absorption and Raman profiles in acetonitrile resulted in a solvent-dephasing time $\tau_1 = (2\pi\Lambda_1)^{-1}$ of about 70 fs, independent of solvent isotopomer and in the range expected for inertial relaxation. However, we found the dephasing to be in the slow modulation regime, so the calculated profiles are much more sensitive to the amplitude D than the frequency Λ. For the most part, we were able to account for the difference in RR intensity between CH_3CN and CD_3CN by using slightly different values of the amplitude D_1: 1216 cm^{-1} in CH_3CN compared to 1272 cm^{-1} in CD_3CN. We speculate that this difference results from the slightly higher collision rate in the protiated solvent, since collisions limit the range of inertial relaxation and the onset of the diffusional regime. In the acetonitrile studies, the slow phase of solvent response (on a ∼0.6 ps time scale) makes a small contribution to the overall calculated profile. However, including the second relaxation enabled reasonable fits to the REPs to be obtained with a fairly consistent set of displacements which were similar in CH_3CN and CD_3CN. Exceptions to this statement arise in the case of lower frequency modes at 231 and 289 cm^{-1}, for which quite different values for the displacements were used in modeling the data for protio- and deuterioacetonitrile. In addition, we had to employ rather large non-Condon corrections to the transition moment in order to obtain calculated REPs that maximize at the correct frequency. We suspect that these problems may be tied to deficiencies in the solvent-dephasing model.

The bimodal solvent-dephasing function in methanol included relaxation on time scales of 60 fs and 0.9 ps. The amplitude of the slow response was found to be twice as large in CH_3OH as in CD_3OD: 1170 vs 550 cm^{-1}. This supports our assignment of the 0.9 ps response to hydroxyl group torsions, which have a larger amplitude in protiomethanol due to higher zero-point energy and weaker hydrogen bonding compared to those in deuterated methanol. More so than in the acetonitrile study, different normal mode displacements had to be employed in modeling the REPs in protio- and deuteriomethanol.

Some our conclusions concerning the effect of isotopic substitution on solvent relaxation have been confirmed by recent time domain experiments.[39−42] Lee et al.[42] reported three-pulse photon echo experiments using the cyanine dye DTTCI in acetonitrile, methanol, and their deuterated derivatives. The shortest relaxation times reported in this study were on the order of 200 fs, and not significantly different in protiated and deuterated derivatives of the same solvent. However, Lee et al. observed signifcant solvent isotope effects on the steady-state fluorescence Stokes shift which suggest that solvent reorganization energy is larger in CH_3OH than that in CD_3OH, while in acetonitrile λ_{solv} is larger in the deuterated solvent. Since λ_{solv} is proportional to the square of the dephasing amplitude, these trends are in accord with our results for betaine-30. Also as in our studies, the absorption spectrum of DTTCI was observed to be independent of solvent isotopomer, even though the fluorescence spectrum and dephasing amplitudes were not.

This leads to an important question: How can the absorption spectrum of betaine-30 be independent of solvent isotope when the Raman intensities are not? Clearly, the same solvent-dephasing function cannot determine both the absorption and Raman cross sections. The breadth of the absorption spectrum depends on solvent fluctuations which are equilibrated to the solute ground electronic state. The solvent motion which decides the Raman intensity, on the other hand, proceeds from a highly nonequilibrium configuration, and the average indicated by the angle brackets in eq 4 is very sensitive to the early inertial relaxation. Similar conclusions were reached in ref 42, where it was concluded that the solvent isotope effect on the Stokes shift of DTTCI results from the fluorescence being faster than the nanosecond solvent relaxation that was observed to depend on solvent isotope; i.e., fluorescence is emitted before solvation is complete. Raman emission is, of course, even faster and therefore more sensitive to solvent isotope effects on the early phase of solvent relaxation.

Solvent dynamics alone cannot account for the mode-dependent solvent isotope effects observed in our experiments. If all vibrational modes see the same solvent response, then similar solvent isotope effects would be observed for all normal modes, in contrast to our results. In addition to mode-dependent dephasing and vibrational relaxation, which are not accounted for in the time-dependent theory, there may also be direct coupling of solute and solvent vibrational modes. Such coupling could be more important for the lower frequency vibrations which are more closely matched to external vibrational frequencies of the solvent.

Does vibrational relaxation occur on the Raman time scale? The question of the entanglement of vibrational and solvent dynamics also arises in time-resolved experiments.[43] For solution-phase chromophores the size of betaine-30, vibrational cooling times are on the order of 10 ps, too slow to affect the Raman intensity. Lower frequency vibrations may undergo subpicosecond population relaxation,[44,45] and the rate of this would depend on solvent isotopomer through energy-matching considerations for the flow of excess vibrational energy from solute to solvent. Intramolecular vibrational redistribution, on the other hand, is at least as fast as inertial solvent relaxation.[34] This is not accounted for in the present theory, but one would expect it to depend on anharmonic coupling within the solute rather than the frequency of solvent-accepting modes. For more insight into these questions, solvent isotope studies of another chromophore are presented in the next section.

3.2. Solvent Dynamical Effects on the Charge-Transfer Transition of an Aqueous Hemicyanine Dye. The structure of 4-[2-(4-dimethylaminophenyl)ethenyl]-1-methylpyridinium (HR, for short, **II** in Figure 3) is typical of many molecules capable of undergoing twisted intramolecular charge transfer (TICT) in the excited electronic state. TICT state formation is often characterized by dual fluorescence, the lower energy emission being red-shifted with increasing solvent polarity due to charge separation associated with internal rotation.[46] Dual fluorescence is not observed in HR, and the absorption and fluorescence spectra are not mirror images. The absorption spectrum is much broader and more sensitive to solvent polarity than the emission and is much broader in aqueous solution than in other polar solvents.[47] Further, the fluorescence quantum yield decreases as solvent polarity increases. This experimental evidence prompted our theoretical[15] and experimental[16] studies of HR in H_2O and D_2O.

We performed semiempirical quantum mechanical calculations on HR and included a cylindrical solvation model to account for solvent polarity. The ground- and excited-state energies and charge distributions were investigated as a function of internal rotation about several bonds, and it was concluded that TICT state formation is likely associated with rotation about the single bond joining the dimethylaniline ring and the central double bond. The charge distribution of HR as a function of this torsion varies more strongly for the excited state than for the ground state and may be responsible for the increased width of the absorption spectrum compared to the fluorescence spectrum. According to our calculations, the excited-state potential surface is not displaced along this torsional coordinate, and there is no evidence of Raman activity for this vibration.

Figure 6 shows RR spectra of HR in H_2O at several excitation freqeuncies, and example REPs are shown in Figure 7. Many of the 18 RR-active normal modes of HR

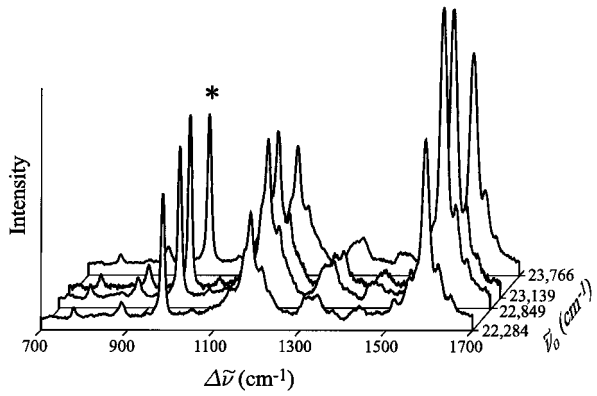

FIGURE 6. Resonance Raman spectra of HR in H_2O. The asterisk marks the Raman band of sulfate ion, used as an internal standard.

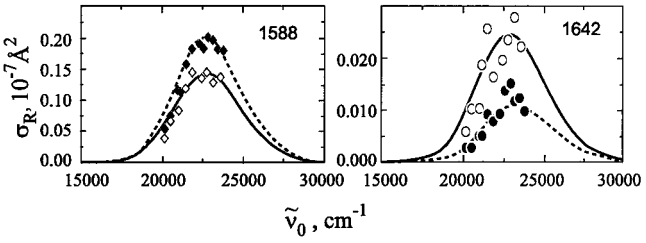

FIGURE 7. Raman excitation profiles for the 1588 and 1642 cm^{-1} modes of HR in H_2O (open symbols) and D_2O (filled symbols). The curves are calculated using time-dependent theory as described in ref 16.

are insensitive to solvent isotopomer, others are stronger in H_2O than in D_2O, and some are more intense in D_2O than in H_2O. There is simply no way to account for these effects by using different solvent-induced dephasing functions in water and heavy water. Further insight was provided by normal coordinate calculations and evaluation of the atomic charge distributions in the ground and excited electronic states. The normal modes most sensitive to solvent isotopomer are those involving motion of atoms which undergo a large change in partial charge between the ground and excited electronic states. The best fits to the experimental absorption and Raman profiles necessitated using different displacements Δ_a for some modes in water and heavy water. Though it is possible that solute−solvent hydrogen bonding is playing some role in this, it is not clear whether the excited-state geometry is really different in the two solvent isotopomers, or whether the different fitted displacements in H_2O and D_2O are compensating for some deficiency in the dephasing model. The absorption and emission spectra of HR are slightly different in H_2O and D_2O. We speculate that solvent−solute coupling of vibrational modes is particularly strong due to fast (∼20 fs) inertial relaxation of water.[39] This time scale τ corresponds to a frequency $\Lambda = (2\pi\tau c)^{-1}$ of about 250 cm^{-1}, which is on the order of a typical torsional mode frequency and could result in coupling of water relaxation to torsional modes. Internal rotation of HR probably contributes to dephasing in addition to that induced by the solvent. Torsional motion associated with formation of the TICT state may contribute to the greater absorption line width in water compared to that in nonaqueous solvent. The absorption and

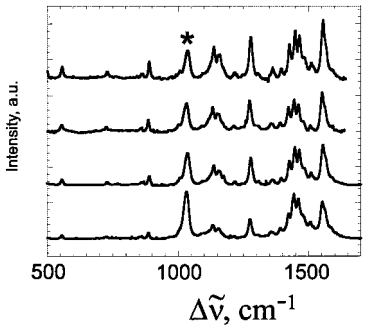

FIGURE 8. Resonance Raman spectra of LDS750 in CH_3OH excited at (from bottom to top) 458, 488, 501, and 514 nm. The asterisk marks a methanol vibration.

emission line widths are slightly narrower in D_2O than in H_2O, as would be expected if part of the width is due to librational motion of the solvent which is coupled to the transition. There is also the possibility that skeletal vibrations of HR in the vicinity of 1600 and 1200 cm^{-1} could couple with the weakly Raman active bending vibration in H_2O and D_2O, respectively. Indeed, the 1642 cm^{-1} mode of HR is more intense in H_2O than in D_2O, and the 1210 cm^{-1} mode is stronger in D_2O than in H_2O, so it is possible that spectral overlap or some sort of resonance coupling could lead to intensity perturbations.[48] However, the 1588 cm^{-1} vibration of HR is significantly more intense in D_2O than in H_2O, and this cannot be a mere consequence of spectral overlap with solvent internal modes. Clearly there are many remaining questions, and it would be enlightening to determine the RR spectra of HR in nonaqueous solution as a function of solvent isotopomer.

3.3. LDS750—Dephasing Controlled by Intramolecular Dynamics. The laser dye LDS750 (**III** in Figure 3) would seem to be an unlikely candidate for a resonance Raman study, but we undertook to observe both the RR and the fluorescence spectra of this dye in methanol and perdeuterated methanol.[17] The experiment is made possible by the fairly large Stokes shift (3200 cm^{-1}), which permits RR spectra to be excited at wavelengths on the blue side of the absorption maximum. Using excitation wavelengths in the range 458−514 nm, the fluorescence still presents a formidable background, but with care it can be fit to a polynomial and subtracted (Figure 8). We found that the Raman intensities of LDS750 are, within error, the same in methanol-h_4 and methanol-d_4; however, the fluorescence yield is about 30% larger in deuterated methanol. Though LDS750 is solvatochromic, it is much less so than betaine-30. Like HR, LDS750 is believed to undergo internal rotation in the excited electronic state, and the emission spectrum is narrower and less sensitive to solvent than the absorption spectrum. It appears that, like HR, LDS750 undergoes excited-state isomerization, and the relaxed excited state has a charge distribution similar to that of the ground state.

A number of time-resolved spectroscopy experiments have probed excited-state dynamics in LDS750.[51−53] Early experiments assigned the 70 fs relaxation in acetonitrile to inertial solvent relaxation, but more recent work suggests that the subpicosecond Stokes shift results from

intramolecular relaxation.[51] Bardeen et al.[52] applied four-wave mixing to uncover a solvent-independent relaxation of LDS750 on a <100 fs time scale. The lack of a solvent isotope effect on the RR intensity supports the conclusion that the dephasing dynamics are controlled by intramolecular relaxation rather than solvent motion. This process, be it isomerization or vibrational relaxation, is distinct from the longer time scale process (about 200 ps in methanol) which precedes relaxed emission. The increased fluorescence intensity in CD_3OD compared to that in CH_3OH results from slower radiationless decay in deuterated methanol, which is in turn a consequence of less favorable Franck−Condon factors for lower frequency solvent-accepting modes. We are led to conclude that the solute exerts an influence on the solvent vibrations, a conclusion supported by transient infrared measurements which observed changes in solvent vibrations following excitation of LDS750.[53]

What is the nature of the ∼100 fs intramolecular process, and how should it be incorporated into the model for the absorption and Raman profiles of LDS750? Vibrational relaxation could influence the RR spectra in our study, since they were excited with several thousand wavenumbers in excess of the origin. Unfortunately, the intrinsic fluorescence prevents RR spectra from being determined on the red side of the absorption maximum, and the working equations of time-dependent theory make no allowance for vibrational relaxation. The possible existence of rotational isomers in the ground electronic state also remains open to question. LDS750 may be a challenging molecule for RR analysis, but our experiments demonstrate how solvent isotopomers can be employed to distinguish intramolecular from solvent reorganization.

4. Related Studies and Future Directions

Some interesting solvent effects on RR intensities have been reported. Phillips et al.[54] observed solvent-dependent Raman intensities in bianthryl even though the absorption spectrum is fairly insensitive to solvent. A few other studies have observed internal reorganization energies which apparently depend on solvent.[55,56] Perhaps some excited-state geometries really are solvent dependent, but if solvent relaxation is not properly accounted for, then the displacements derived from RR intensity will be wrong. Quantum calculations of electronic transitions of solvated molecules will help to address these questions. INDO calculations on betaine-30[31] suggest that the longest wavelength transition in methanol is the transition to the S_2 state, rather than that to S_1. This would account for the very different displacements we obtained for betaine-30 in methanol as opposed to those in acetonitrile. As a counter example, we determined REPs for the solvatochromic complex $[Ru(NH_3)_4bipyridine]^{2+}$ in DMSO and methanol[57] and performed quantum calculations to make qualitative assignments of the electronic states.[58] In this complex, the displacements and overall Raman cross sections are not very solvent sensitive, but as a result of solvent-mediated configuration mixing, preresonance enhancement from a higher lying state is much stronger in methanol than in DMSO. Even though solvent relaxation in methanol is very distinct from that in DMSO, these differences do not show up in the Raman spectrum, perhaps because fast population relaxation is the dominant damping factor.

When the resonance Raman spectrum is influenced by solvent isotope, the effect can be used to advantage to determine improved models for solvent-induced dephasing. Work along these lines is in progress in our laboratory. The possible connection between nonlinear solvent dynamics and solvatochromism will also be explored by examining a range of chromophore probes. Increased use of solvent isotopomers in time-resolved experiments would lead to better understanding of chromophore−solvent dynamics. Though the ideal chromophore probe should report (rather than perturb) solvation dynamics, by choosing molecules with large Stokes shifts for RR experiments, the solute is more likely to couple strongly to the solvent. Proper treatment of this coupling and the influence of vibrational relaxation will be necessary in order to correctly extract the intramolecular dynamics from the Raman excitation profiles.

The support of the National Science Foundation is gratefully acknowledged. It is a pleasure to acknowledge the talented students and co-workers who have contributed to this work: Yaping Zong, Xuan Cao, Doug Daniel, John Streiff, Dan Edwards, Mark Wall, and especially, Fritz Knorr. I am indebted to all of them for their hard work and dedication and for making these studies enjoyable.

References

(1) Lee, S.-Y.; Heller, E. J. Time-dependent theory of Raman scattering. *J. Chem. Phys.* **1979**, *71*, 4777.
(2) Heller, E. J.; Sundberg, R. L.; Tannor, D. Simple aspects of Raman scattering. *J. Phys. Chem.* **1982**, *86*, 1822.
(3) Heller, E. J. Semiclassical way to molecular spectroscopy. *Acc. Chem. Res.* **1981**, *14*, 368.
(4) Tannor, D. J.; Heller, E. J. Polyatomic Raman scattering for general harmonic potentials. *J. Chem. Phys.* **1982**, *77*, 202.
(5) Myers, A. B.; Mathies, R. A. Resonance Raman intensities: A probe of excited-state structure and dynamics. In *Biological Applications of Raman Spectroscopy*; Spiro, T. G., Ed.; Wiley: New York, 1987; Vol. 2, p 1.
(6) See, for example, the recent volume of Advances in Chemical Physics: *Electron Transfer: From Isolated Molecules to Biomolecules*; Jortner, J., Bixon, M., Eds.; Advances in Chemical Physics 107; Wiley: New York, 1999.
(7) Myers, A. B. Relating absorption, emission, resonance Raman spectra with electron-transfer rates in photoinduced charge-transfer systems. *Chem. Phys.* **1994**, *180*, 215.
(8) Walker, G. C.; Åkesson, E.; Johnson, A. E.; Levinger, N. E.; Barbara, P. F. Interplay of solvent motion and vibrational excitation in electron-transfer kinetics. *J. Phys. Chem.* **1992**, *96*, 3728.
(9) Reid, P. J.; Barbara, P. F. Dynamic solvent effect in betaine-30 electron transfer. *J. Phys. Chem.* **1995**, *99*, 3554.
(10) Åkesson, E.; Walker, G. C.; Barbara, P. F. Dynamic solvent effects on electron transfer in the inverted regime. *J. Chem. Phys.* **1991**, *95*, 4188.
(11) Zusman, L. D. Outer sphere electron transfer in polar solvents. *Chem. Phys.* **1980**, *49*, 295.
(12) Sumi, H.; Marcus, R. A. Dielectric relaxation and intramolecular electron transfers. *J. Chem. Phys.* **1986**, *84*, 4272.
(13) Zong, Y.; McHale, J. L. Resonance Raman study of solvent dynamics in electron transfer I. Betaine-30 in CH_3CN and CD_3CN. *J. Chem. Phys.* **1997**, *106*, 4963.
(14) Zong, Y.; McHale, J. L. Resonance Raman study of solvent dynamics in electron transfer II. Betaine-30 in CH_3OH and CD_3OD. *J. Chem. Phys.* **1997**, *107*, 2920.

(15) Cao, X.; Tolbert, R. W.; McHale, J. L.; Edwards, W. D. Theoretical study of solvent effects on the intramolecular charge transfer of a hemicyanine dye. *J. Phys. Chem. A* **1998**, *102*, 2739.
(16) Cao, X.; McHale, J. L. Resonance Raman study of solvent dynamics on the spectral broadening and intramolecular charge transfer of a hemicyanine dye in aqueous solution. *J. Chem. Phys.* **1998**, *109*, 1901.
(17) Knorr, F. J.; Wall, M. H.; McHale, J. L. Investigation of solvent isotope effects on the Raman and fluorescence intensity of LDS750 in CH_3OH and CD_3OD. *J. Phys. Chem. A* **2000**, *104*, 9494.
(18) Mukamel, S. *Nonlinear Optical Spectroscopy*; Oxford: New York, 1995.
(19) Sue, J.; Yan, Y. J.; Mukamel, S. Raman excitation profiles of polyatomic molecules in condensed phases. *J. Chem. Phys.* **1986**, *85*, 462.
(20) Mukamel, S. Solvation effects in four-wave mixing and spontaneous Raman and fluorescence lineshapes of polyatomic molecules. *Adv. Chem. Phys.* **1988**, *70*, 165.
(21) Carter, E. A.; Hynes, J. T. Solvation dynamics for an ion pair in a polar solvent. *J. Chem. Phys.* **1991**, *94*, 5961.
(22) Rosenthal, S. J.; Xie, X.; Du, M.; Fleming, G. R. Femtosecond solvation dynamics in acetonitrile. *J. Chem. Phys.* **1991**, *95*, 4715.
(23) Maroncelli, M.; Fleming, G. R. Picosecond solvation dynamics of coumarin 153. *J. Chem. Phys.* **1987**, *86*, 6221.
(24) Stratt, R. M.; Maroncelli, M. Nonreactive dynamics in solution: the emerging view of solvation dynamics and vibrational relaxation. *J. Phys. Chem.* **1996**, *100*, 12981.
(25) Cho, M.; Fleming, G. R. Electron transfer and solvent dynamics. *Adv. Chem. Phys.* **1999**, *107*, 311.
(26) Cho, M.; Yu J.-Y.; Nagasawa, Y.; Passino, S. A.; Fleming, G. R. The integrated photon echo and solvation dynamics. *J. Phys. Chem.* **1996**, *100*, 11944.
(27) de Boeij, W. P.; Pshenichnikov, M. S.; Wiersma, D. A. System-bath correlation function probed by conventional time-gated stimulated photon echo. *J. Phys. Chem.* **1996**, *100*, 11806.
(28) Reichardt, C. Solvatochromic dyes as solvent polarity indicators. *Chem. Rev.* **1994**, *92*, 2319.
(29) Lobaugh J.; Rossky, P. J. Computer simulation of the excited state dynamics of betaine-30 in acetonitrile. *J. Phys. Chem. A* **1999**, *103*, 9432.
(30) Mente, S. R.; Maroncelli, M. Computer simulations of the solvatochromism of betaine-30. *J. Phys. Chem. B* **1999**, *103*, 7704.
(31) Alencastro, R. B.; Da Motta Neto, J. D.; Zerner, M. C. Solvent effects on the electronic spectrum of betaine-30. *Int. J. Quantum Chem. Chem. Symp.* **1994**, *28*, 361.
(32) Liptay, W.; Dumbacher, B.; Weisenberger, H. Die Beeinflussung der optischen Absorption von Molekülen durch ein electrisches Feld. *Z. Naturforsch. Teil A* **1968**, *23*, 1613.
(33) McMorrow, D.; Lotshaw, W. T. Intramolecular dynamics in acetonitrile probed with femtosecond Fourier transfrom spectroscopy. *J. Phys. Chem.* **1991**, *95*, 10395.
(34) Horng, M. L.; Gardecki, J. A.; Papazyan, A.; Maroncelli, M. Subpicosecond measurements of polar solvation dynamics: coumarin 153 revisited. *J. Phys. Chem.* **1995**, *99*, 17311.
(35) Ladanyi, B. M.; Liang, Y. Q. Interaction-induced contributions to polarizability anisotropy relaxation in polar liquids. *J. Chem. Phys.* **1995**, *103*, 6325.
(36) Passino, S. A.; Nagasawa, Y.; Joo, T.; Fleming, G. R. Three-pulse echo peak shift studies of polar solvation dynamics. *J. Phys. Chem. A* **1997**, *101*, 725.
(37) Bingemann, D.; Ernsting, N. P. Femtosecond solvation dynamics determining the band shape of stimulated emission from a polar styryl dye. *J. Chem. Phys.* **1995**, *102*, 2691.
(38) Skaf, M. S.; Fonseca, T.; Ladanyi, B. M. Wave vector dependent dielectric relaxation in hydrogen-bonding liquids. *J. Chem. Phys.* **1993**, *98*, 8929.
(39) Zolotov, B.; Gan, A.; Fainberg, B. D.; Huppert, D. Resonance heterodyne optical Kerr spectroscopy of solvation dynamics in water and D_2O. *Chem. Phys. Lett.* **1997**, *265*, 418.
(40) Pal, H.; Nagasawa, Y.; Tominaga, K.; Kumazaki, S.; Yoshihara, K. Deuterium isotope effect on solvation dynamics. *J. Chem. Phys.* **1995**, *19*, 7758.
(41) Wynne, K.; Galli, C.; Hochstrasser, R. M. Femtosecond intermolecular vibrational motion in pyrrole. *Chem. Phys. Lett.* **1992**, *193*, 17.
(42) Lee, S.-H.; Lee, J.-H.; Joo, T. Deuterium isotope effects on the solvation dynamics of a dye molecule in methanol and acetronitrile. *J. Chem. Phys.* **1999**, *110*, 10969.
(43) Book, L. D.; Scherer, N. F. Wavelength-resolved stimulated photon echoes: Direct observation of ultrafast intramolecular vibrational contributions to electronic dephasing. *J. Chem. Phys.* **1999**, *111*, 792.
(44) Elsaesser, T.; Kaiser, W. Vibrational and vibronic relaxation of large polyatomic molecules in liquids. *Annu. Rev. Phys. Chem.* **1991**, *42*, 83.
(45) Miller, R. J. Vibrational energy relaxation and structural dynamics of heme proteins. *Annu. Rev. Phys. Chem.* **1991**, *42*, 581.
(46) Strehmel, B.; Seifert, H.; Rettig, W. Photophysical properties of fluorescence probes. *J. Phys. Chem. B* **1997**, *101*, 2232.
(47) Görner, H.; Kuhn, H. J. Cis−trans isomerization of stilbenes and stilbene-like molecules. *Adv. Photochem.* **1995**, *19*, 1.
(48) Daniel, D. C.; McHale, J. L. Intensity perturbations from vibrational resonance coupling in isotropic Raman spectra of neat liquids and solutions. *J. Chem. Phys.* **1997**, *106*, 1699.
(49) Castner, E. W., Jr.; Maroncelli, M.; Fleming, G. R. Subpicosecond resolution studies of solvation dynamics in polar aprotic and alcohol solvents. *J. Chem. Phys.* **1987**, *86*, 1090.
(50) Cho, M.; Rosenthal, S. J.; Scherer, N. F.; Ziegler, L. D.; Fleming, G. R. Ultrafast solvation dynamics: Connection between time resolved fluorescence and optical Kerr measurements. *J. Chem. Phys.* **1992**, *96*, 5033.
(51) Kovalenko, S. A.; Ernsting, N. P.; Ruthmann, J. Femtosecond Stokes shift in styryl dyes: Solvation or intramolecular relaxation? *J. Chem. Phys.* **1997**, *106*, 3504.
(52) Bardeen, C. J.; Rosenthal, S. J.; Shank, C. V. Ultrafast solvation processes in polar liquids probed with large organic molecules. *J. Phys. Chem. A* **1999**, *103*, 10506.
(53) Lian, T.; Kholodenko, Y.; Hochstrasser, R. M. Infrared probe of solvent response to ultrafast solvation process. *J. Phys. Chem.* **1995**, *99*, 2456.
(54) Scholes, G. D.; Fournier, T.; Parker, A. W.; Phillips, D. Solvation and intramolecular reorganization in 9,9′ bianthryl. *J. Chem. Phys.* **1999**, *111*, 5999.
(55) Yamaguchi, T.; Kimura, Y.; Hirota, N. Solvent and solvent density effects on the spectral shifts and the bandwidths of absorption and resonance Raman spectra of phenol blue. *J. Phys. Chem. A* **1997**, *101*, 9050.
(56) Kimura, Y.; Hirota, N. Effect of solvent density and species on the static and dynamic fluorescence Stokes shifts of coumarin 153. *J. Chem. Phys.* **1999**, *111*, 5474.
(57) Streiff, J.; McHale, J. L. Resonance Raman study of solvatochromic electronic transitions of $[Ru(NH_3)_4bipyridine]^{+2}$ in methanol and dimethylsulfoxide. *J. Chem. Phys.* **2000**, *112*, 841.
(58) Streiff, J.; McHale, J. L.; Edwards, W. D. Investigation of the solvatochromic electronic transitions of $[Ru(NH_3)_4bipyridine]^{+2}$ *Chem. Phys. Lett.* **1999**, *312*, 369.

AR000007L